

Experimental and theoretical investigation of the temperature dependence of La_2CuO_4 sublattice magnetization

V. D. Doroshev, V. N. Krivoruchko, M. M. Savosta, A. A. Shestakov, and D. A. Yablonskiĭ

Donetsk Physicotechnical Institute, Ukrainian Academy of Sciences

(Submitted 27 May 1991)

Zh. Eksp. Teor. Fiz. **101**, 190–202 (January 1992)

The temperature dependence sublattice magnetization of La_2CuO_4 was determined precisely by the ^{139}La NQR method at temperatures from 4.2 K to $T_N \geq 315$ K. The results were processed in the framework of the four-sublattice model in the approximation of noninteracting spin waves. Comparison of the theoretical calculations with the experimental results yielded the effective magnetic fields representative of La_2CuO_4 . It is shown that the noninteracting-spin-wave approximation describes the experimental dependence satisfactorily all the way to $T^* \leq (5/6) T_N$.

I. INTRODUCTION

The antiferromagnetism of copper ions in CuO_2 planes, being one of the most important features of HTSC compounds, is of increasing interest to researchers. A crucial role in the explanation of the magnetic properties of the crystal is played by the values of the effective magnetic fields and by the character of interaction between the magnetic ions. It is established by now that a Heisenberg interaction takes place in the planes CuO_2 of Cu^{2+} ions in La_2CuO_4 and $\text{YBa}_2\text{Cu}_3\text{O}_6$ with a strong spatial anisotropy of the exchange interaction (see, e.g., Ref. 1). The parameters of the intralayer exchange interaction have been determined quite definitely.¹ Approximate estimates exist^{1,2} for anisotropic interactions. At the same time, the role of the anisotropy of the interactions is significantly higher in low-dimensional multisublattice magnets,³ owing to weakening of the interlayer exchange. A direct method of determining the magnetic parameters is an experimental investigation of the dynamics and thermodynamics of the system and comparison of the results with the predictions of a theory that takes the real structure of the crystal into account.

A distinguishing feature of HTSC compounds is that these antiferromagnets (AFM) are low-dimensional, so that the laws of variation of the magnetization, susceptibility, heat capacity, and other characteristics are all different from those for three-dimensional magnets. Thus, the exchange modes of the spin oscillations constitute an inalienable and most important property of such systems, and determine their dynamics and thermodynamics.³ An experimental check of the theoretical results on magnetoresonant properties of HTSC compounds meets at present with serious difficulties.⁴ Particular importance attaches therefore to a comparison of theory with experiment in thermodynamics. Nuclear magnetic and quadrupole (NQR) methods have also turned out to be productive here. (A survey of NQR studies of the properties of HTSC compounds can be found in Ref. 5.)

The present paper is devoted to an experimental and theoretical investigation of the temperature dependence of the magnetization of Cu^{2+} ions in La_2CuO_4 . The spin-echo method was used to study the NQR of ^{139}La ($I = \frac{7}{2}$, $\nu/2\pi = 601.44$ Hz/Oe, $Q = 0.21 \cdot 10^{-24}$ cm²) of stoichiometric La_2CuO_4 with $T_N \geq 315$ K. The temperature depend-

ence of the relative sublattice magnetization was determined precisely. The results were reduced in the framework of the 4-sublattice model in the non-interacting-spin-wave approximation. The manifestations of anisotropic interactions in the dynamics and thermodynamics of the system were analyzed. Comparison of the theoretical calculations with the experimental results yielded the values of the effective fields that characterize La_2CuO_4 .

II. EXPERIMENTAL PROCEDURE

The temperature dependence of the sublattice magnetization of antiferromagnetic $\text{La}_2\text{CuO}_{4+\delta}$ were determined by using various methods: the Mössbauer effect (ME), magnetic neutron diffraction, muon spin rotation, and NQR. Earlier investigations were aimed at observing the antiferromagnetic order, and yielded subsequently quite reliable quantitative results. It is generally accepted that the most precise measurements of the relative sublattice magnetization $M(T)/M(0)$ of AFM can be made by the ME method and by high-precision resonance procedures as NMR and NQR.

In our opinion, in the case of $\text{La}_2\text{CuO}_{4+\delta}$ the results with the smallest scatter of the data are those of EM (Ref. 6) and NQR (Ref. 7) investigations. Even these results, however, cannot be used for a reliable comparison with the conclusions of spin-wave theory at temperatures $T < 100$ K, in view of either the lack of low-temperature data⁶ or the appreciable errors⁷ comparable with the magnetization variations. In addition, it cannot be assumed beforehand that in the case of $\text{La}_2\text{CuO}_{4+\delta}$ the ME data reflect adequately the behavior of the temperature dependence of the sublattice magnetization. The measure of magnetization in the ME method is the value of the contact (Fermi) hyperfine field at the ^{57}Fe nucleus (~ 490 kOe at 4.2 K) induced by the proper $3d$ shell of the magnetically ordered iron-ion dopant replacing the Cu^{2+} ion in the $\text{La}_2\text{CuO}_{4+\delta}$ matrix. The Fe–Cu exchange interaction, while antiferromagnetic, can in this case differ substantially from the one for the Cu–Cu bonds, and this should inevitably lead to significant systematic errors. For example, it was observed⁸ in studies of the temperature dependence of the hyperfine interaction of the field at the ^{57}Fe nuclei in $\text{RBa}_2\text{Cu}_3\text{O}_z$ that the Fe–Cu exchange is much weaker than the Cu–Cu exchange. It is appropriate to note

here that the Heisenberg behavior of the Cu^{2+} ion in La_2CuO_4 is apparently unique. Thus, the related compounds La_2NiO_4 and La_2CoO_4 obtained by replacing the copper ion by Ni^{2+} ($S=1$) or Co^{2+} ($s=3/2$), are already Ising AFM.

NQR investigations of the sublattice magnetization in $\text{La}_2\text{CuO}_{4+\delta}$ do not require introduction of impurities and can in principle consist of measurements of either the proper hyperfine fields of Cu^{2+} ions at the $^{63,65}\text{Cu}$ nuclei or of the local magnetic field \mathbf{H}_{loc} (μ_{Cu}) induced at the ^{139}La nuclei of the nominally diamagnetic La^{3+} ions by surrounding Cu^{2+} ions with moments μ_{Cu} . Unfortunately, the most direct first method cannot be realized in view of the strong shortening of the nuclear relaxation time with rise of temperature.⁹ In addition, small deviations from the pure spin state of the Cu^{2+} ion can lead to an appreciable orbital contribution to the field at the $^{63,65}\text{Cu}$ nuclei, which masks the behavior of the contact field due to the spin moment (all the way to sign reversal, e.g., Ref. 10).

In the case of NQR of ^{139}La , the relaxation times are long enough all the way to T_N , and the lines are narrow, so that a small scatter of the data can be achieved. This procedure, however, is indirect, and an analytic estimate can lead to the conclusion that systematic errors are not significant. Calculations in the point-dipole mode show that the dipole contribution H_{dip} to the field \mathbf{H}_{loc} at the La^{3+} ion amounts to $\sim 60\%$ at $\mu_{\text{Cu}} \approx 0.6\mu_B$. Since the carrier density in $\text{La}_2\text{CuO}_{4+\delta}$ is low, the contribution lack is due to indirect hyperfine interactions.

One can estimate by direct summation the effect exerted on the principal dipole contribution by thermal expansion of the crystal and by the change of the degree of orthorhombicity with change of temperature. A complete set of crystallographic data¹¹ is available for the $\text{La}_2\text{CuO}_{4.032}$ compound and is indicative of the changes of the lattice and of the coordinates in the general lattice positions on going from 15 K to room temperature. Calculation shows that the lattice sum for H_{dip} decreases in this temperature interval only by a small amount, $\sim 0.6\%$, whereas the experimentally observed decrease of the local field is $\sim 42\%$. It is unfortunately impossible to obtain such simple estimates for the indirect hyperfine field induced via the $\text{La}^{3+}-\text{O}^{2-}-\text{Cu}^{2+}$ chains. Taking into account, however, the relative small value of this contribution and the very weak dependence on the interatomic distances, obtained for example for the $\text{Fe}^{3+}-\text{O}^{2-}-\text{Fe}^{3+}$ chain in orthoferrites,¹² it can be assumed that the systematic error in the measurement of the induced sublattice magnetization, by the ^{139}La NQR method at 300 K, does not exceed 1–2%.

The NQR spectrum of ^{139}La in $\text{La}_2\text{CuO}_{4+\delta}$ has a complex structure and consists of 9 lines located for $T \rightarrow 0$ K in the frequency range 2–20 MHz. This form of the spectrum is determined by the simultaneous interaction of the quadrupole moment of a nucleus having a spin $I=7/2$ with an electric field gradient (EFG) having no axial symmetry in the $Cmca$ orthorhombic phase, and of its magnetic moment with \mathbf{H}_{loc} arbitrarily oriented relative to the principal axes of the EFG tensor.^{7,13} It was established^{7,13} that for $T \rightarrow 0$ K, in full accord with the crystal symmetry, \mathbf{H}_{loc} is located in the bc plane making an angle $\theta \approx 78^\circ$ with the EFG-tensor principal axis which is also located in this plane. The parallel

component of \mathbf{H}_{loc} turns out to be small ($H_{\parallel} = \cos\theta \cdot H_{\text{loc}} \approx 0.2 H_{\text{loc}}$), while the parallel one is decisive ($H_{\perp} = \sin\theta \cdot H_{\text{loc}} \approx 0.98 H_{\text{loc}}$). The degree of orthorhombicity decreases with temperature (a transition to the tetragonal phase $I4/mmm$ takes place at $T \approx 540$ K, so that $H_{\parallel} \rightarrow 0$).

It was customary in all the known measurements of the relative magnetization to use two pairs of high-frequency lines $\nu_5-\nu_8$ (in the frequency range 12–20 MHz as $T \rightarrow 0$ K), in view of their high intensity. The splittings ($\nu_8 - \nu_7$) and ($\nu_6 - \nu_5$) in these pairs (the transitions $7/2 \rightarrow 5/2$ and $5/2 \rightarrow 3/2$) are determined, however, by the small H_{\parallel} component, so that the measurement accurately is substantially lowered. In addition, identification of $M(T)/M(0)$ with $H_{\parallel}(T)/H_{\parallel}(0)$ leads inevitably to systematic errors since the angle θ decreases with temperature. In the present study we measured the frequencies of the weak lines $\nu_1-\nu_4$ (in the range 5–8 MHz as $T \rightarrow 0$ K) for the transitions $\pm 3/2 \rightarrow \Phi_{\pm 1/2}$, the splitting of which is governed not only by H_{\parallel} but mainly by the leading component H_{\perp} . This is a much more complicated experimental task, but raises by almost an order of magnitude the magnetization-measurement accuracy. In addition, the approximation $M(T)/M(0) = H_{\text{loc}}(T)/H_{\text{loc}}(0)$, where $H_{\text{loc}} = \sqrt{H_{\parallel}^2 + H_{\perp}^2}$, excludes all the systematic errors due to the aforementioned temperature dependence of the orthorhombicity.

The components H_{\parallel} and H_{\perp} should in principle be determined from the experimental line frequencies by numerical diagonalization of the nuclear spin Hamiltonian.⁷ Recognizing, however, the reliably established fact⁷ that the EFG asymmetry parameter is small ($\eta = 0.01 \pm 0.01$), we have used for the NQR frequencies the simple equations derived¹⁴ in first-order perturbation theory for an axisymmetric EFG:

$$\nu_{1,2} = \nu_{7/2 \rightarrow 5/2} \mp \frac{3}{2} \frac{\gamma}{2\pi} H_{\parallel} - \frac{1}{2} \frac{\gamma}{2\pi} [H_{\parallel}^2 + (4H_{\perp})^2]^{1/2}, \quad (1)$$

$$\nu_{3,4} = \nu_{5/2 \rightarrow 3/2} \mp \frac{3}{2} \frac{\gamma}{2\pi} H_{\parallel} + \frac{1}{2} \frac{\gamma}{2\pi} [H_{\parallel}^2 + (4H_{\perp})^2]^{1/2}.$$

The local-field components are defined as

$$\frac{\gamma}{2\pi} H_{\parallel} = (\nu_4 - \nu_3 + \nu_2 - \nu_1)/6, \quad (2)$$

$$\frac{\gamma}{2\pi} [H_{\parallel}^2 + (4H_{\perp})^2]^{1/2} = (\nu_4 + \nu_3 - \nu_1 - \nu_2)/2.$$

We estimated the inadequacy of the assumed description of the spectrum by comparing $(\nu_4 - \nu_3)$ with $(\nu_2 - \nu_1)$ and $(\nu_4 - \nu_1)$ with $(\nu_3 - \nu_2)$. The corresponding frequency differences agreed within the limits of the errors of the NQR frequency measurement.

A polycrystalline $\text{La}_2\text{CuO}_{4+\delta}$ specimen¹⁵ was used. It was heat treated after synthesis in a vacuum of 10^{-2} Torr at 900°C for 12 hours. This heat treatment reduces the oxygen excess above stoichiometry, as evidenced by the strong narrowing of the line widths from 100–150 kHz (synthesized specimen) to 30 kHz. The specimen Néel temperature determined from the susceptibility maximum was 315 K. The narrowing of the lines was an additional contribution to the relative-magnetization measurement accuracy.

TABLE I.

№	T, K	M(T)/M(0)	№	T, K	M(T)/M(0)
1	4,2	1,000	18	240,0	0,675
2	16,0	0,997	19	254,9	0,638
3	29,0	0,994	20	265,1	0,610
4	40,1	0,989	21	275,1	0,580
5	50,0	0,983	22	279,9	0,564
6	59,9	0,975	23	285,0	0,546
7	70,0	0,966	24	290,1	0,527
8	80,0	0,955	25	295,1	0,506
9	90,0	0,945	26	298,0	0,491
10	100,0	0,934	27	300,9	0,477
11	100,1	0,934	28	304,0	0,460
12	120,1	0,906	29	307,1	0,440
13	140,1	0,877	30	310,1	0,421
14	159,9	0,840	31	312,0	0,404
15	179,6	0,804	32	313,9	0,385
16	200,0	0,764	33	316,1	0,365
17	218,6	0,722	34	318,0	0,347

Note. Here $M(0)$ is the sublattice magnetization at 4.2 K.

The NQR was registered using a two-pulse vacuum echo with analog storage and with spectrum recording by linear scanning of the generator frequency. At each fixed temperature the spectrum was recorded many times and statistically processed in a computer. The accuracy of the measured resonant frequencies is estimated at $\pm (2-10)$ kHz, depending on the temperature. A free-flow helium cryostat was used to maintain the temperature in the 4.2–300 K range. The temperature was measured accurate to ± 0.5 K. Table I lists the measured values of $M(T)/M(4.2)$.

III. THEORY

The magnetic structure of La_2CuO_4 is shown in Fig. 1. A symmetry analysis of the La_2CuO_4 structure is reported in a number of papers.¹⁶⁻¹⁹ Using these results, the Hamiltonian of the model can be expressed in the form

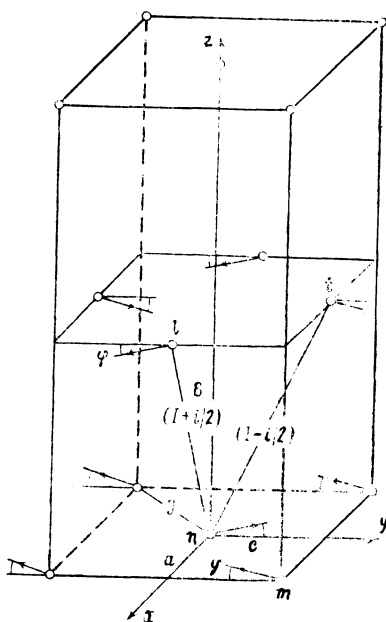


FIG. 1. Magnetic structure of La_2CuO_4 .

$$\begin{aligned}
 H = \frac{1}{2} \sum_{\mathbf{n}} \left[J \sum_{\mathbf{m}} \mathbf{S}_{\mathbf{n}} \mathbf{S}_{\mathbf{m}} + \sum_{\mathbf{l}} (I+i/2) \mathbf{S}_{\mathbf{n}} \mathbf{S}_{\mathbf{l}} + \sum_{\mathbf{t}} (I-i/2) \mathbf{S}_{\mathbf{n}} \mathbf{S}_{\mathbf{t}} \right. \\
 \left. - \sum_{\mathbf{m}} A_z \mathbf{S}_{\mathbf{n}}^z \mathbf{S}_{\mathbf{m}}^z - \sum_{\mathbf{m}} d (\mathbf{S}_{\mathbf{n}}^y \mathbf{S}_{\mathbf{m}}^z - \mathbf{S}_{\mathbf{n}}^z \mathbf{S}_{\mathbf{m}}^y) \right. \\
 \left. - \sum_{\mathbf{l}} A (\mathbf{S}_{\mathbf{n}}^x \mathbf{S}_{\mathbf{l}}^x - \mathbf{S}_{\mathbf{n}}^y \mathbf{S}_{\mathbf{l}}^y) + \sum_{\mathbf{t}} A (\mathbf{S}_{\mathbf{n}}^x \mathbf{S}_{\mathbf{t}}^x - \mathbf{S}_{\mathbf{n}}^y \mathbf{S}_{\mathbf{t}}^y) \right]. \quad (3)
 \end{aligned}$$

Here $\mathbf{S}_{\mathbf{n}}$ is the spin operator at an arbitrary site \mathbf{n} , and the subscripts \mathbf{m} , \mathbf{l} , and \mathbf{t} number the nearest neighbors of the site \mathbf{n} in the xy , yz , and xz planes. The parameter J is indicative of the intralayer exchange interaction; owing to rhombic distortions, the exchange interfield interactions are determined by two parameters, $I \pm i/2$, with i small to the extent that the rhombic distortions are small (see Fig. 1). We assume below that $J \gg I \gg i$.

The anisotropic interactions A_z and A are preserved also in the tetragonal phase and are apparently among the basic relativistic interactions. The intrafield exchange-relativistic interaction of the Dzyaloshinskii type, d , leads to noncollinearity of the magnetic moments in the layer. Recall that the magnetization vectors of neighboring layers are antiparallel (see, e.g., Ref. 16). We left out of (3), besides an anisotropy of rhombic origin, $A_y \mathbf{S}_{\mathbf{n}}^y \mathbf{S}_{\mathbf{m}}^y$ with $A_y \sim |a-c|/(a+c) \ll A_z$, also terms of relativistic and exchange-relativistic origin, which contribute to the spectrum only for wave vectors parallel to the CuO_2 planes and located close to the Brillouin-zone boundary. We assume that so integral a characteristic of the system as sublattice magnetization is sufficiently well described in the chosen approximation. These questions are discussed in greater detail in Sec. IV.

The spin structure of La_2CuO_4 (Fig. 1) has four sublattices and is weakly noncollinear. To describe such a structure in the general case it is necessary to introduce four magnetic sublattices. In the absence of a magnetic field, however, the investigated system (3) has supersymmetry, so that it can be described in the context of the method of expanded translational symmetry.²⁰ Indeed, the Hamiltonian (3) and

the thermodynamic-equilibrium state (Fig. 1) are invariant to the operations

$$\mathbf{T}_{nm}U_{2z}, \mathbf{T}_{n1}U_{2x}, \mathbf{T}_{n1}U_{2y}, \quad (4)$$

where \mathbf{T}_{nm} , \mathbf{T}_{n1} , and \mathbf{T}_{nt} are operators of translations between the corresponding atoms, while U_{2x} , U_{2y} and U_{2z} are operators of second-order spin-rotations about the axes x , y , and z , respectively. The last circumstance is the condition for the validity of the method of expanded translational symmetry,²⁰ which permits description of the 4-sublattice AFM (3) in the language of a single magnetic sublattice.

Following Ref. 20 and taking (4) into account, we change from the operators \mathbf{S}_n , \mathbf{S}_m , \mathbf{S}_1 , \mathbf{S}_t to the corresponding operators σ_n , σ_m , σ_1 , σ_t , using the equations

$$\begin{aligned} \sigma_n &= (\mathbf{S}_n^x; \mathbf{S}_n^y; \mathbf{S}_n^z); \quad \sigma_1 = (\mathbf{S}_1^x; -\mathbf{S}_1^y; -\mathbf{S}_1^z); \\ \sigma_m &= (-\mathbf{S}_m^x; -\mathbf{S}_m^y; \mathbf{S}_m^z); \quad \sigma_t = (-\mathbf{S}_t^x; \mathbf{S}_t^y; -\mathbf{S}_t^z). \end{aligned}$$

The Hamiltonian (3) takes in terms of the operators σ the form

$$\begin{aligned} H &= \frac{1}{2} \sum_n \left[\sum_m \mathbf{J} (-\sigma_n^x \sigma_m^x - \sigma_n^y \sigma_m^y + \sigma_n^z \sigma_m^z) \right. \\ &\quad + \sum_1 (I+i/2) (\sigma_n^x \sigma_1^x - \sigma_n^y \sigma_1^y - \sigma_n^z \sigma_1^z) \\ &\quad + \sum_t (I-i/2) (-\sigma_n^x \sigma_t^x + \sigma_n^y \sigma_t^y - \sigma_n^z \sigma_t^z) - \sum_m A_z \sigma_n^z \sigma_m^z \\ &\quad - \sum_m d (\sigma_n^y \sigma_m^z + \sigma_n^z \sigma_m^y) - \sum_1 A (\sigma_n^x \sigma_1^x + \sigma_n^y \sigma_1^y) \\ &\quad \left. - \sum_t A (\sigma_n^x \sigma_t^x + \sigma_n^y \sigma_t^y) \right]. \end{aligned}$$

As expected, it has an additional invariance to the translations

$$\mathbf{T}_{nm}, \mathbf{T}_{n1}, \mathbf{T}_{nt}. \quad (5)$$

Since the initial structure is noncollinear, we change over to the local coordinate frame for the operators σ_n (it is already the same for all sites):

$$\begin{aligned} \sigma_n^x &= \xi_n^x; \quad \sigma_n^y = \xi_n^z \cos \varphi + \xi_n^y \sin \varphi, \\ \sigma_n^z &= \xi_n^z \sin \varphi - \xi_n^y \cos \varphi. \end{aligned}$$

After changing from spin operators to Bose operators a_n and a_n^+ with the aid of the Holstein-Primakoff representation, we obtain a standard-form Hamiltonian $H = E_0 + H_1 + H_2 + \dots$, where E_0, H_1, H_2, \dots are forms of zeroth, first, second, etc., orders in the Bose operators a_n^+ and a_n . Minimizing E_0 with respect to φ , we get

$$\operatorname{tg}(2\varphi) = \frac{d}{2J}, \quad (6)$$

which agrees, naturally, with Refs. 18 and 19. Following this, H_1 vanishes. Changing from the operators a_n^+ and a_n to their spatial Fourier transforms [taking into account the new translational symmetry (5)] we obtain for the Hamiltonian quadratic in the Bose operators

$$H = \sum_{\mathbf{k}} [A_{\mathbf{k}} a_{\mathbf{k}}^+ a_{\mathbf{k}} + \frac{1}{2} B_{\mathbf{k}} (a_{\mathbf{k}}^+ a_{-\mathbf{k}}^+ + a_{-\mathbf{k}} a_{\mathbf{k}})], \quad (7)$$

$$\begin{aligned} A_{\mathbf{k}} &= 2J + 2i + 4A + 2d \sin(2\varphi) \\ &\quad - [A_z - d \sin(2\varphi)] \cos(ak_x) \cos(ck_y) \\ &\quad - (A + 2I - i) \cos(ck_y) \cos(bk_z) - A \cos(bk_z) \cos(ak_x), \\ B_{\mathbf{k}} &= -[2J - A_z + d \sin(2\varphi)] \cos(ak_x) \cos(ck_y) \\ &\quad - A \cos(ck_y) \cos(bk_z) - (A - 2I - i) \cos(bk_z) \cos(ak_x). \end{aligned}$$

The spin wave spectrum (7) is described by the standard equation:

$$H_2 = \sum_{\mathbf{k}} E_{\mathbf{k}} c_{\mathbf{k}}^+ c_{\mathbf{k}}, \quad E_{\mathbf{k}} = (A_{\mathbf{k}}^2 - B_{\mathbf{k}}^2)^{1/2} \quad (8)$$

and is defined in an expanded Brillouin zone. Here $c_{\mathbf{k}}^+$ and $c_{\mathbf{k}}$ are the quasiparticle operators. Oscillations with wave numbers $(0,0,\pi/b)$ and $(0,\pi/c,0)$ correspond to homogeneous acoustic modes, and those with wave vectors $(0,0,0)$ and $(0,\pi/c,\pi/b)$ to homogeneous exchange modes. The corresponding activation energies are

$$\begin{aligned} E_{a1} &= 4(2JA + d^2/4)^{1/2}, \quad E_{a2} = 4[J(A + A_z/2)]^{1/2}, \\ E_{o1} &= 4(Ji + d^2/4)^{1/2}, \quad E_{o2} = 4[J(i + A + A_z/2)]^{1/2} \end{aligned} \quad (9)$$

and coincide with those obtained in Ref. 19. The spin-wave spectrum reveals a clearly pronounced quasi-two-dimensional character with weak dispersion perpendicular to the CuO_2 layers ($\mathbf{k} \parallel \text{OZ}$) and strong dispersion for wave vectors parallel to the layers ($\mathbf{k} \perp \text{OZ}$) (see Fig. 2).

Since the magnetic interactions are quasi-two-dimensional, the magnetic-ordering temperature T_N is much lower than the "exchange temperature" J . In the calculation of the thermodynamic characteristics in the non-interacting spin-wave approximation the main contribution is made therefore by the low-energy part of the spectrum, corresponding to small vicinities of the wave vectors $\mathbf{k}_1 = (0,0,k_z)$ and $\mathbf{k}_2 = (0,\pi/c,k_z)$ with $0 \leq bk_z \leq +\pi$. The spin-wave vector can be expressed in these regions as

$$\begin{aligned} E_j &= (a_j - b_j \cos \kappa_{\parallel} + 4J^2 \kappa_{\perp}^2)^{1/2}, \\ \kappa_{\parallel} &= bk_z, \quad \kappa_{\perp}^2 = (ak_x)^2 + (ck_y)^2. \end{aligned} \quad (10)$$

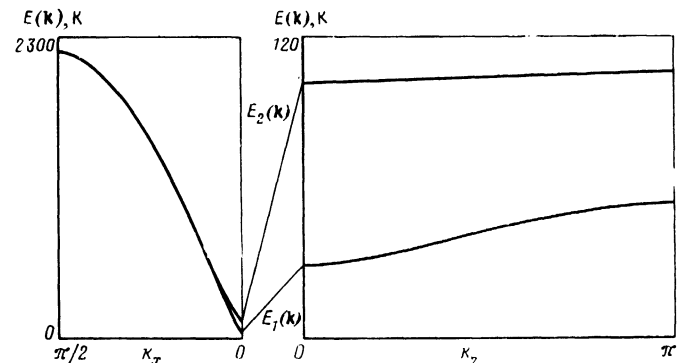


FIG. 2. Spin-wave spectrum of La_2CuO_4 at $J = 1100$ K, $i = 0.045$ K, $A = 0.08$ K, $A_z = 1$ K, $d = 6$ K (set 12 of Table II).

The subscripts $j = 1, 2$ indicate the vicinity of the region \mathbf{k}_1 or \mathbf{k}_2 in which the given expansion is made, while the coefficients a_j and b_j , with allowance for the condition $J \gg I$, are equal to

$$a_1 = 8J[2A + i + d \sin(2\varphi)], \quad b_1 = 8J(2A - i), \\ a_2 = 8J(2A + A_2 + i), \quad b_2 = 8Ji.$$

Using (8), we can obtain an expression for the sublattice magnetization of the system in the approximation of noninteracting spin waves; this expression is $M(T) = g\mu_B \langle S_z \rangle$, where

$$\langle S_z \rangle = S - \frac{1}{N} \sum_{\mathbf{k}} \langle a_{\mathbf{k}} + a_{\mathbf{k}} \rangle = S - \frac{1}{N} \sum_{\mathbf{k}} \frac{A_{\mathbf{k}} n_{\mathbf{k}}}{E_{\mathbf{k}}} \\ + \frac{1}{2} \left[1 - \frac{1}{N} \sum_{\mathbf{k}} \frac{A_{\mathbf{k}}}{E_{\mathbf{k}}} \right] = S - \Delta S_0 - \Delta S(T). \quad (11)$$

The term ΔS_0 describes the quantum cancellation of the spin, and it is known²¹ that in the limiting case of noninteracting layers we have $\Delta S_0 = 0.1965$. As noted above, the main contribution to the term $\Delta S(T)$ is made by small vicinities of the regions of \mathbf{k}_1 and \mathbf{k}_2 , i.e., $\Delta S(T) = \Delta S_1(T) + \Delta S_2(T)$ where, after integrating twice,

$$\Delta S_j(T) = - \frac{T}{2\pi^2 J} \int_0^{\pi} \ln \left\{ 1 - \exp \left[- \frac{[a_j - b_j \cos(\kappa_{\parallel})]^{1/2}}{T} \right] \right\} d\kappa_{\parallel}. \quad (12)$$

The asymptotic behavior of the sublattice magnetization (12) at low and high temperatures agrees with the well

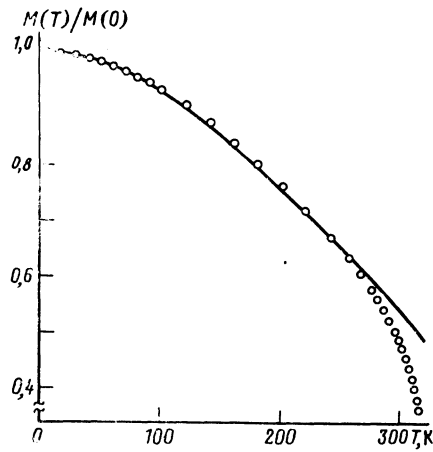


FIG. 3. Experimental (points) and theoretical ($J = 1100$ K, $i = 0.045$ K, $A = 0.08$ K, $A_2 = 1$ K, $d = 6$ K) dependence of the sublattice magnetization of La_2CuO_4 .

known results $\Delta S(T) \sim T^2$ and $\Delta S(T) \approx T \ln T$. The integrals, however, can be analytically calculated only in a number of limiting cases. Thus, analytic expressions can be obtained for the sublattice magnetization in the isotropic model ($A_z = A = d = 0$) or neglecting in (3) the terms that depend on the orthorhombic distortions ($i = d = 0$). There are no indications for choosing one of these approximations for La_2CuO_4 . The remaining data were therefore obtained with a computer.

IV. DISCUSSION OF RESULTS

The magnetic parameters of the system can be obtained by comparing the experimental data with the numerical results. Figure 3 shows a theoretical curve obtained for the

TABLE II.

No.	J	i	A	A_2	d	E_{a1}	E_{o1}	E_{a2}	E_{o2}	T^*
1	880	0,03	0,4	1,5	6	107	24	127	129	280
2	1000	0,01	0,05	6,5	6	42	17	230	230	250
3	1000	0,01	0,1	3	6	58	17	160	160	260
4	1000	0,01	0,2	1,4	6	81	17	120	121	260
5	1000	0,01	0,4	0,15	6	114	17	87	88	270
6	1000	0,1	0,05	2,5	6	42	42	144	150	260
7	1000	0,1	0,1	1,5	6	58	42	117	123	260
8	1000	0,1	0,2	0,6	6	81	42	89	98	270
9	1100	0,01	0,05	2,5	6	44	18	151	152	250
10	1100	0,01	0,1	1,2	6	61	18	111	112	260
11	1100	0,01	0,2	0,4	6	85	18	84	85	260
12	1100	0,045	0,08	1	6	54	31	101	105	260
13	1100	0,1	0,05	1	6	44	44	98	107	250
14	1100	0,1	0,1	0,5	6	61	44	78	89	260
15	1100	0,1	0,2	0,05	6	85	44	63	76	250
16	1200	0,01	0,05	1,1	6	45	18	107	108	240
17	1200	0,01	0,1	0,5	6	63	18	82	83	243
18	1200	0,01	0,2	0,1	6	88	18	69	71	220
19	1200	0,1	0,05	0,4	6	45	45	69	82	245
20	1200	0,1	0,1	0,1	6	63	45	54	69	240
21	1250	0,02	0,08	0,4	6	58	23	75	77	220
22	1000	0,001	0,3	1,3	0	98	4	123	123	260
23	1000	0,001	0,5	0,09	0	126	4	93	93	270
24	1100	0,7	0,02	0	0	27	111	19	113	260
25	1300	0,32	0,006	0,03	7,8	22	83	21	84	215
26	1300	0,03	0,05	0,04	7	48	29	38	46	215
27	1350	0,05	0,05	0,1	10,6	51	39	46	57	215

Note. All the parameters are given in deg. K.

parameter values $J = 1100$ K; $i = 0.045$ K; $A = 0.08$ K; $A_z = 1$ K; $d = 6$ K (set 12 of Table II). The results agree here with the measurements within the limits of experimental error, all the way to $T^* \approx 260$ K. It must be borne in mind at the same time that in quasi-low-dimensional systems the weak three-dimensionalizing exchange and the anisotropy play interchangeable roles in the formation of the initial magnetic order (see, e.g., Ref. 23 and the citations therein). As a result, the magnetic-interaction parameters cannot be uniquely chosen.

Table II lists several sets of magnetic parameters for La_2CuO_4 for which the results of the theoretical computations agree with the experimental data within the limits of experimental error all the way to the temperatures T^* . The table lists also the theoretical AFMR frequencies (9) corresponding to a given choice of parameters. Each set is in a certain sense "critical," i.e., when one of the parameters deviates from the indicated values the theoretical $M(T)$ curve deviates noticeably from the experimental points.

Analysis of the results shows that the best agreement between theory and experiment is reached if the intralayer exchange interaction J takes on values in the interval (1000 ± 100) K. A systematic discrepancy between the experimental and theoretical data, exceeding the experimental error, is observed for set No. 1 of Table II with the low value $J = 880$ K in the low-temperature region $T < 100$ K. At higher values of the intralayer exchange ($J \geq 1200$ K, see sets Nos. 16–21 and 25–27)¹⁾ the temperature interval in which the theoretical and experimental $M(T)$ dependences agree decreases.

The calculation results are shown for each of the sets 2–8 ($J = 1000$ K, 9–15 ($J = 1100$ K and 16–20 ($J = 1200$ K) at two values of the weak interlayer exchange interaction ($i = 0.01$ K and $i = 0.1$ K). We have tried here to satisfy the following additional condition: the interlayer anisotropy A must not exceed the intralayer A_z . Note that the parameter A_z decreases when the parameter A increases. A similar dependence is observed also for any other pair of parameters. As a result the range of variation of the parameters A and A_z decreases with increase of J .

The parameter d enters in the theory [see Eq. (7)] only in combination with the small noncollinearity angle (6) of the structure. As a result, the theoretical $M(T)$ curve is not very sensitive to changes of d . The parameters i , A , and A_z are mutually interchangeable, and are therefore difficult to determine uniquely. Note that the experimental $M(T)$ dependence can be satisfactorily described also in the isotropic limit (A , A_z , $d \ll i$ —set 24) and neglecting the orthorhombic distortions (i , $d \ll A$, A_z —sets 22 and 23). Satisfactory agreement with experiment is reached also when the values of the weak three-dimensionalizing exchange are comparable with one of the anisotropy constants. Such solutions are lost when the asymptotic dependences are used.

The presently available data on the AFMR frequencies are quite ambiguous. A broad resonance was obtained²⁵ at 9 cm^{-1} and interpreted by the authors as the frequency of one of the spectrum modes. This conclusion is refuted in Ref. 4, where it is shown that the observed absorption is not connected with oscillations of the La_2CuO_4 spin system. At the same time, Peters *et al.*²⁶ determined from neutron-scattering results the activation of the spin-wave modes $(9 \pm 2$

cm^{-1} and 22 ± 4 cm^{-1}), one of which is close to the results of Ref. 25. It would undoubtedly be of interest to observe the exchange modes, which have unusual properties in La_2CuO_4 (Refs. 18, 19). First, as seen from Table II, they have a high probability of being located below the acoustic modes; furthermore, this type of excitation should vanish in sufficiently strong fields when a transition to the two-sublattice AFM phase is observed.^{27,28}

Returning the analysis of the $M(T)$ dependence, we note also that owing to the large values we obtained for the spin-wave activation energies (9) which determine the transition from the low-temperature to the high-temperature asymptote of $M(T)$, it is impossible to determine at $T < T_N$ the temperature interval in which the high-temperature $M(T) \sim T \ln T$ dependence is valid. At the same time, in the temperature range 4.2 K $< T < 70$ K, the experimental data are also approximated with sufficient accuracy by the quadratic (low-temperature) asymptotic relation.

As seen from Fig. 3 and Table II, the approximation of noninteracting spin-waves describes satisfactorily the experimental data and in a considerably larger temperature range ($T^* \lesssim \frac{5}{6} T_N$) than in ordinary three-dimensional magnets, owing to the substantial difference between the three-dimensional-ordering temperature and the intralayer-exchange energy, and even near $T_{N(C)}$ the occupation numbers are not small only in the case of long-wave magnons. The interaction effects for the latter are small.^{29,30} As a result, the range of validity of the spin-wave approximation, in $T/T_{N(C)}$ relative units, is wider than in the three-dimensional case. This circumstance is well confirmed experimentally for two-sublattice layered AFM (see Ref. 31 and the citations therein). A manifestation of this physical behavior is also the insignificant role of the kinematic interaction of magnons in quasi-low-dimensional magnets.³²

It is instructive, from the methodological point of view, to compare the experimental sublattice-magnetization temperature dependence obtained by the Mössbauer effect on ⁵⁷Fe nuclei⁶ and the NQR data listed in Table I. The most detailed results are given in Ref. 6 for a specimen annealed in an argon atmosphere, with a maximum-susceptibility temperature $T_m = 280$ K; the same time we used a specimen annealed in vacuum with a much higher temperature, $T_m = 315$ K. A reliable comparison of the data is possible only in terms of the relative temperature T/T_N , but this calls for knowledge of the magnetic-ordering temperatures.

Exact measurement of T_N is made difficult by the fact that coexistence of antiferromagnetic and paramagnetic phases is observed near the order-disorder transition point both in the sample of Ref. 6 and in our sample, and the transition itself is apparently of first order.¹⁵ We have therefore compared our data as functions of both T/T_m and T/T_N , assuming for our sample the extrapolated value $T_N = 325$ K (Ref. 15), and for the sample of Ref. 6 $T_N \approx 300 \pm 5$ K. In both cases the $M(T)/M(0)$ plot corresponding to the Mössbauer procedure lies substantially lower than the plot obtained by the NQR method. The systematic difference between the values of $M(T)/M(0)$ in the region $T/T_N \approx 0.7$ amount to $\sim 11\%$, which is many times larger than the relative error of the two procedures. By the same token, a conclusion drawn in Ref. 8 for another layered AFM, $\text{YBa}_2\text{Cu}_3\text{O}_2$, that the Fe-Cu exchange is substantially

weaker than the Cu–Cu exchange, is confirmed qualitatively also for $\text{La}_2\text{CuO}_{4+\delta}$. In the case of La_2CuO_4 , however, this effect is not as strongly pronounced because for $R\text{Ba}_2\text{Cu}_3\text{O}_z$ the relative-magnetization differences reached $\sim 25\%$ at $T/T_N \approx 0.6\text{--}0.7$ (Ref. 8).

V. CONCLUSION

The spin-echo method was used to study the ^{139}La NQR of stoichiometric La_2CuO_4 with $T_N \geq 315$ K. The temperature dependence of the relative sublattice magnetization of La_2CuO_4 was determined precisely from the Zeeman splitting of the NQR spectrum for the $\pm \frac{3}{2} \rightarrow \Phi_{\pm 1/2}$ transition. The results were processed in the framework of the 4-sublattice model in the approximation of noninteracting spin waves. Account was taken of the following: the intralayer exchange J of the nearest copper ions; the Dzyaloshinskii interaction d and the interlayer exchange i due to the orthorhombic distortions; anisotropic interactions that are conserved in the tetragonal phase, and those of uniaxial anisotropies of intralayer (A_z) and interlayer (A) origin. At the parameter values in Table II, satisfactory agreement is obtained between the experimental and theoretical results all the way to $T \approx 260$ K.

The authors thank A. A. Bush for supplying the sample and S. F. Ivanov and V. A. Borodin for help with the measurements.

¹⁾ The parameters of set 25 were proposed in Ref. 2, and the values for J and d for set No. 26 in Table II were taken from Ref. 24.

¹⁾ Yu. A. Izyumov, N. M. Plakida, and Yu. N. Skryabin, *Usp. Fiz. Nauk* **159**, 621 (1989) [*Sov. Phys. Usp.* **32**, 1060 (1989)].

²⁾ M. D. Kuz'min, A. I. Popov, and A. K. Zvezdin, *Phys. Lett. A* **139**, 419 (1989).

³⁾ A. I. Zvyagin, M. I. Kobets, and V. N. Krivoruchko, *Zh. Eksp. Teor. Fiz.* **89**, 2298 (1985) [*Sov. Phys. JETP* **63**, 1328 (1985)].

⁴⁾ S. G. Kaplan, T. W. Toh, A. J. Sievers *et al.*, *Phys. Rev. B* **40**, 5190 (1989).

⁵⁾ N. E. Ainbinder, in *Surveys of High-temperature Superconductivity* [in Russian], No. 3, 3–35 (1990).

⁶⁾ H. Tang, G. Xiao, A. Sing *et al.*, *J. Appl. Phys.* **67**, 4518 (1990).

⁷⁾ H. Nishihara, H. Yasuoka, T. Shimizu *et al.*, *J. Appl. Phys.* **56**, 4559 (1987).

⁸⁾ I. Nowik, G. Kaindl, E. R. Bauminger *et al.*, *Sol. St. Commun.* **74**, 957 (1990).

⁹⁾ T. Tsuda, T. Shimizu, H. Yasuoka *et al.*, *J. Phys. Soc. Jpn.* **57**, 2908 (1989).

¹⁰⁾ L. D. Khoi, M. Rotter, and R. Krishnan, *Phys. Stat. Sol. (a)* **12**, 569 (1972).

¹¹⁾ C. Chaillont, S. W. Cheong, Z. Fisk *et al.*, *Physica C* **158**, 183 (1989).

¹²⁾ V. D. Doroshev, S. F. Ivanov, A. N. Molchanov, and A. S. Moskvina, *Pis'ma Zh. Eksp. Teor. Fiz.* **45**, 583 (1987) [*JETP Lett.* **45**, 743 (1987)].

¹³⁾ V. D. Doroshev and M. M. Savosta *ibid.* **50**, 328 (1989) [**50**, 363 (1989)].

¹⁴⁾ A. Abragam, *Principles of Nuclear Magnetism*, Oxford, 1961.

¹⁵⁾ V. A. Borodin, V. D. Doroshev, Yu. M. Ivanchenko, M. M. Savosta, and A. E. Filippov, *Pis'ma Zh. Eksp. Teor. Fiz.* **52**, 1073 (1990) [*JETP Lett.* **52**, 469 (1990)].

¹⁶⁾ M. A. Kastner, R. J. Birgenau, T. R. Thurston *et al.*, *Phys. Rev. B* **38**, 6631 (1988).

¹⁷⁾ A. S. Borovik-Romanov, A. I. Buzdin, N. M. Kreines, and S. S. Krotov, *Pis'ma Zh. Eksp. Teor. Fiz.* **47**, 600 (1988) [*JETP Lett.* **47**, 697 (1988)].

¹⁸⁾ V. G. Bar'yakhtar, V. M. Loktev, and D. A. Yablonskii, *Physica C* **156**, 667 (1988).

¹⁹⁾ V. G. Bar'yakhtar, V. M. Loktev, and D. A. Yablonskii, *SFKhT 2*, No. 11, 16 (1989).

²⁰⁾ A. L. Alistratov and D. A. Yablonskii, *Zh. Eksp. Teor. Fiz.* **94**, No. 11, 194 (1988) [*Sov. Phys. JETP* **67**, 2285 (1988)].

²¹⁾ M. E. Lines, *J. Phys. Chem. Solids* **31**, 101 (1970).

²²⁾ V. L. Berezinskii and A. Ya. Blank, *Zh. Eksp. Teor. Fiz.* **64**, 725 (1973) [*Sov. Phys. JETP* **37**, 369 (1973)].

²³⁾ V. A. Slyusarev and R. P. Yankelevich, *Fiz. Nizk. Temp.* **3**, 1175 (1977) [*Sov. J. Low Temp. Phys.* **3**, 570 (1977)].

²⁴⁾ T. Tho, T. R. Thurston, and N. W. Breyer, *Phys. Rev. B* **38**, 905 (1988).

²⁵⁾ R. T. Collins, Z. Schlesinger, M. W. Shafer, and T. R. McGuire, *ibid.* **B 37**, 5817 (1988).

²⁶⁾ C. J. Peters, R. J. Birgenau, N. A. Kastner *et al.*, *ibid.* **B 37**, 9761 (1988).

²⁷⁾ T. Thio, R. J. Birgenau, S. Y. Chen *et al.*, *Physica C* **162–164**, part II, 1301 (1989).

²⁸⁾ V. G. Baryakhtar, V. M. Loktev, V. A. L'vov, and D. A. Yablonskii, *SFKhT 2*, 59 (1989).

²⁹⁾ F. Lyson, *Phys. Rev.* **102**, 1217 (1956).

³⁰⁾ A. B. Harris, D. Kumar, B. I. Halperin, and P. S. Hohenberg, *Phys. Rev. B* **3**, 961 (1971).

³¹⁾ R. J. Birgenau, H. J. Guggenheim, and G. Shirane, *ibid.* **B 9**, 304 (1973).

³²⁾ V. N. Krivoruchko, *Teor. Mat. Fiz.* **71**, No. 2, 290 (1987).

Translated by J. G. Adashko